Geophys. J. Int. (2001) **144,** 481–494

Unusual thermomagnetic behaviour of haematites: neoformation of a highly magnetic spinel phase on heating in air

Cor B. de Boer and Mark J. Dekkers

Palaeomagnetic Laboratory 'Fort Hoofddijk', Utrecht University, Faculty of Earth Sciences, Budapestlaan 17, 3584 *CD Utrecht, the Netherlands. E-mail: dekkers@geo.uu.nl*

Accepted 2000 September 12. Received 2000 August 3; in original form 1999 September 16.

SUMMARY

The formation of traces of a magnetic phase with a Curie point of 470–475 °C is detected during routine thermomagnetic analysis of various haematite types without significant isomorphous substitution. Using heating and cooling rates of 10° min^{-1}, the formation temperature can be as low as 400 °C for synthetic haematite samples, whereas higher temperatures, 700–800 °C, are required for natural samples. The new phase appears to be persistent to prolonged heating at 1000 °C and has a cubic spinel structure with a unit cell length $a_0 = 0.8350 \pm 0.0005$ nm, similar to pure maghemite. This suggests that the reverse reaction of the γ-$Fe_2O_3 \rightarrow \alpha$-$Fe_2O_3$ transformation can occur under appropriate conditions. The low T_C of this particular maghemite variety suggests that the vacancy (and/or cation) ordering over the magnetic sublattices is different from usually occurring maghemite. In accordance with Takei & Chiba (1966), who also reported a pure maghemite variety with identical T_C, a cation-deficient spinel structure with part of the vacancies on tetrahedral sites is suggested. Thermally activated release of incorporated hydroxyl groups would trigger the formation of maghemite traces on the surface of well-crystalline haematite planes. Citrate–bicarbonate–dithionite extraction results support the idea that the maghemite is fine-grained and surficial on the haematite because low-field susceptibility values decrease according to the behaviour of fine-grained maghemite particles. The formation of traces of this highly magnetic mineral during routine step-wise thermal demagnetization or during annealing haematite at high temperatures may seriously affect NRM measurements or may be erroneously taken as haematite's defect moment.

Key words: haematite, maghemite, rock magnetism, thermomagnetic analysis.

1 INTRODUCTION

Under oxidizing conditions and ambient pressure, haematite (α-Fe_2O_3), the hexagonal polymorph of ferric oxide, is thermodynamically the most stable of all naturally occurring pure iron oxide phases over a broad temperature range. Its dissociation temperature in air is *c.* 1450 °C (*cf.* Zdujic *et al.* 1998) and its melting point is *c.* 1565 °C (*cf.* Morrish 1994). The α-Fe_2O_3 phase diagram at 1 atm suggests 1000 °C as the lowest temperature at which local reduction in air can occur (*cf.* Dunlop 1971). Gardner *et al.* (1963) measured the electrical conductivity of haematites and reported that molecular oxygen loss, leading to the formation of metal excess, occurred only upon firing stoichiometric α-Fe_2O_3 in air above 1000 °C. Below *c.* 1000 °C, however, no oxygen loss was detected. Indeed, apart from minor structural improvements and possible changes in grain-size and shape due to sintering, no phase changes are reported for pure haematite after annealing at high temperatures (900–1100 °C) in air. This procedure is therefore commonly used in rock-magnetic studies to improve the crystallinity of haematites synthesized at low temperatures and to anneal out the defect moment introduced in freshly crushed haematite particles (e.g. Dunlop 1971; Bucur 1978; Fysh & Clark 1982).

Although being metastable, the other common iron oxide forms can usually persist for long time at normal sub-aerial conditions (even on a geological timescale), because of sluggish kinetics. The oxidation rate of Fe^{2+}-bearing iron oxides (magnetite, Fe_3O_4, and the cation-deficient spinels of the $Fe^{3+}Fe^{2+}_{1-z}Fe^{3+}_{1+2z/3}\square_{z/3}O_4$ series with $0 < z < 1$, where $\square$ denotes the vacancies), however, increases with temperature and with decreasing particle size. In addition, the inversion of the cubic γ-Fe_2O_3 polymorph, maghemite, to the stable hexagonal form is a thermally activated process. Consequently, laboratory heating in air of mineral concentrates of all known naturally

occurring pure iron oxides (and thus also of all pure iron sulphides and oxyhydroxides) eventually results in the formation of stable α-Fe_2O_3.

On a laboratory timescale, in the dry state and at ambient pressure, metastable γ-Fe_2O_3 commonly inverts to stable α-Fe_2O_3 at approximately 350 °C. Reported inversion temperatures, however, are highly variable and may range from $\approx$250 °C up to $\approx$900 °C (e.g. Bernal *et al.* 1957; Wilson 1961; Kachi *et al.* 1963; Özdemir & Banerjee 1984; Özdemir & Dunlop 1988; Özdemir 1990; Dunlop & Özdemir 1997), depending on the origin of the maghemite, its crystallinity, impurity content, degree of residual Fe^{2+}, and morphological properties such as particle size and shape.

In general, the γ-$Fe_2O_3 \rightarrow \alpha$-$Fe_2O_3$ transformation has been held to be irreversible. Meillon *et al.* (1995), however, reported the existence of a direct phase transformation from haematite to maghemite by the mechanical action of prolonged (>25 days) wet grinding in ethanol. The grinding process was characterized by the presence of a shearing component exerted on the α-Fe_2O_3 particles. According to the authors, the required rearrangements in the oxygen framework (hexagonal close-packing to cubic close-packing) and in the iron coordination ($^{VI}Fe^{3+}$ in haematite to partially $^{IV}Fe^{3+}$ in maghemite) would be accomplished by this shearing component. X-ray diffraction patterns obtained on the resulting γ-Fe_2O_3 phase showed superstructure reflections diagnostic of long-range ordering of vacancies over octahedral interstices (see Section 2). The inversion temperature lies around 425 °C.

Finch & Sinha (1957) detected the $\alpha \rightarrow \gamma$ transformation under conditions somewhat more realistic from a rock-magnetic point of view. These authors observed in an electron-diffraction study the formation of epitaxial maghemite outgrowths on pure haematite particles on heating above $\approx$700 °C. According to the authors, the γ-Fe_2O_3 was created via an intermediate metastable haematite-like phase (named β-Fe_2O_3 by them), previously formed at 500 °C. This rare β-phase would be characterized by additional reflections which are forbidden for the space group of haematite. It has, however, an oxygen-ion framework and unit cell identical to α-Fe_2O_3, but probably differs from normal haematite by having some cations on tetrahedral interstices similar to the β-Al_2O_3 (bixbyite) structure, as observed by Bragg *et al.* (1931). Finch & Sinha (1957) showed that this proposed structure for β-Fe_2O_3 results in a ferrimagnetic phase. Blackman & Kaye (1960), however, seriously questioned the existence of this intermediate phase. The γ-Fe_2O_3 phase formed during the experiments of Finch & Sinha (1957) showed an unusually high thermal stability as it persisted even after prolonged heating at 900 °C. Their results showed that the α-Fe_2O_3 to γ-Fe_2O_3 transformation may occur under suitable conditions, but an appropriate mechanism to explain the unusual phase transition could not be found. Moreover, the vacancy distribution (see Section 2) and magnetic properties of this maghemite type were not determined.

From a palaeomagnetic point of view, the possible formation of even a small amount of these ferrimagnetic phases is a matter of serious concern in studies of haematite-bearing sediments and rocks. The formation of the β-phase during routine thermal demagnetization treatment before reaching the crucial unblocking temperature segment of normal remanent magnetizations residing in haematite could be an important source of noise, hampering the determination of the characteristic remanent magnetization carried by haematite. Furthermore, the magnetic properties of minute traces of the γ-phase developed during annealing haematite at high temperatures may erroneously be ascribed to the defect moment of haematite. To this end, a description is needed of those haematite types which are susceptible to the $\alpha \rightarrow \gamma$ transition, together with a magnetic characterization of the reaction products, in order to recognize the occurrence of the process.

We measured the thermomagnetic behaviour of various haematite types with basically no isomorphous substitution, to induce the unusual $\alpha \rightarrow \gamma$ transformation and to get a better insight into the appropriate conditions necessary to cause this phase transition. The technique used, that is, the monitoring of the (saturation) magnetization of a sample as a function of temperature, is very sensitive to heating-induced chemical and/or structural changes, in particular if magnetic changes from a weakly anti-ferromagnetic phase (α-Fe_2O_3) to strongly ferrimagnetic phases (β-Fe_2O_3 and γ-Fe_2O_3) are involved. The detection limit of the $M_{(s)}$ monitoring technique is much lower than other structure-sensitive analysing techniques; the creation of minute traces, at least $\approx$0.05 per cent for γ-Fe_2O_3, is readily reflected in irreversible heating and cooling runs during thermomagnetic analysis. Moreover, the specific Curie temperature of the newly created phase may reveal important information about the vacancy ordering over the octahedral and tetrahedral lattice interstices.

2 CRYSTAL STRUCTURE AND ROCK-MAGNETIC BACKGROUND

2.1 Haematite

Haematite crystallizes in the corundum structure (e.g. Blake *et al.* 1966; Lindsley 1976a). The unit cell parameters are $a_{hex} = 0.50340$ nm and $c_{hex} = 1.3752$ nm for stoichiometric haematite (*cf.* Schwertmann & Cornell 1991). The space group is $R\bar{3}c$. In the corundum structure, the oxygen layers are stacked in an AB-sequence parallel to the (0001) basal plane forming an almost ideal hexagonal-close-packed (hcp) lattice. The O^{2-} layers (OL) alternate with layers of octahedrally coordinated Fe^{3+} cations. In haematite, only two-thirds of the available cation sites are occupied because of charge balance considerations (note that vacant sites are implicit in the stoichiometry, and should not be confused with vacancies). The iron ions are arranged regularly, thereby forming sixfold rings within each Fe plane (*cf.* Cornell & Schwertmann 1996). The succession of Fe ions along the (0001) plane is Fe^{3+}:OL:Fe^{3+}:OL:□:OL:Fe^{3+}:OL:□ and so on (*cf.* O'Reilly 1984).

The spin configuration of haematite above the Morin transition is basically anti-ferromagnetic. The magnetic moments of the Fe^{3+} ions lie in the basal (0001) plane orthogonal to the *c*-axis (e.g. Shull *et al.* 1951). Within these (0001) planes the magnetic spins are coupled parallel, but anti-parallel coupling exists between adjacent layers of cations. The cation arrangement in adjacent layers is equivalent so that an overall anti-ferromagnetic structure results. Haematite, however, possesses a weak ferromagnetic moment due to a slight canting of the atomic spins out of exact anti-parallelism (Dzyaloshinsky 1958). This so-called canted moment lies in the basal plane perpendicular to the sublattice magnetizations (Shull *et al.* 1951), and is generally reported to be $\approx$0.3–0.4 $Am^2\,kg^{-1}$ (e.g. Haigh 1957; Flanders & Remeika 1965; Dunlop & Özdemir 1997). In

addition, haematite may have another weak magnetic moment referred to as the 'defect moment'. This more variable moment is thought to reside, at least partly, in an ordered structure of imperfections or impurities in the crystal lattice. Because of its origin, part of this moment is susceptible to heat treatment.

The strong magnetic interactions between Fe atoms on alternating sublattices are reflected in haematite's high magnetic disordering temperature. The Néel temperature (T_N) of pure haematite is commonly reported as $\approx 680\ ^\circ C \pm 5\ ^\circ C$ (e.g. Morrish 1994 and references therein). It is generally assumed that the canting of the sublattices and the anti-ferromagnetic ordering within the sublattice vanish simultaneously. The shapes of the thermomagnetic curves for different types of haematite are described in De Boer & Dekkers (1998).

2.2 Maghemite

Maghemite has the same chemical composition as haematite but like magnetite it crystallizes in the spinel structure, which generally has a $Fd\bar{3}m$ space group. In fact, maghemite can be considered as a non-stoichiometric defect magnetite with incomplete spinel cation site occupancy (Waychunas 1991). A cubic unit cell parameter of $a_0 \approx 0.833$–0.835 nm is usually quoted for maghemite, compared to $a_0 = 0.8396$ nm for magnetite (Lindsley 1976a).

The spinel structure consists of a framework of cubic close-packed (ccp) anion layers (*cf.* O'Reilly 1984). The O^{2-} layers may be seen forming (111) planes of a face-centred cubic (fcc) lattice stacked orthogonal to the cube diagonal [111] direction in an ABC-sequence. The oxygen framework encloses tetrahedral (fourfold coordination) as well as slightly larger octahedral (sixfold coordination) interstices for cations, often referred to as the A and B positions, respectively. In a spinel structure, normally one out of three of the occupied interstices are tetrahedrally coordinated with oxygen and two out of three are octahedrally coordinated. In the cation-deficient spinel structure of maghemite, however, only five out of six of the total available positions are filled by Fe^{3+}, the remaining positions being vacancies. The chemical formula for maghemite written as spinel is thus $Fe_{2.67}\square_{0.33}O_4$. The arrangement of those vacancies appears to be very variable, and is still somewhat controversial. Therefore, what is referred to as 'maghemite' actually comprises various different phases, characterized by a different positioning of the vacancies (Pecharromán *et al.* 1995; Eggleton *et al.* 1988). The vacancies could occur in either octahedral sites or mixed over both tetrahedral and octahedral sites. The presence of a stable maghemite with only tetrahedral vacancies has been discounted by Lindsley (1976a,b).

Most experimental evidence supports the tendency for the vacancies to occupy octahedral sites only (e.g. Armstrong *et al.* 1966; Haneda & Morrish 1977; Greaves 1983; Boudeulle *et al.* 1983; Coey 1987; Collyer *et al.* 1988). Three different varieties of maghemite with completely filled tetrahedral spinel sites are generally accepted. The structures are characterized by a different degree of long-range crystal order of the vacancies (Braun 1952; Van Oosterhout & Rooijmans 1958; Haneda & Morrish 1977; Smith 1979; Greaves 1983; Boudeulle *et al.* 1983; Collyer *et al.* 1988; Eggleton *et al.* 1988; Pecharromán *et al.* 1995). The atomic coordinates of these three idealized crystal structures are summarized by Pecharromán *et al.* (1995) in his Table 1. The maghemite varieties characterized by a totally random, a partly ordered and a totally ordered vacancy distribution have a face-centred cubic, a primitive cubic and a tetragonal structure, respectively. The respective space groups are $Fd\bar{3}m$, $P4_132$ and $P4_32_12$. Vacancy ordering can be particularly evident in X-ray diffraction, where maghemites with vacancy ordering show typical superstructure lines (extra reflections) that are inconsistent with the face-centred cubic system, and thus can be used to distinguish between maghemite and magnetite in addition to differences in a_0.

Takei & Chiba (1966) concluded from their high saturation magnetization value obtained on epitaxially grown single crystals of maghemite (MgO substrate) that part of the vacancies should occupy tetrahedral interstices. Weber & Hafner (1971), Annertsen & Hafner (1973) and Ramdani *et al.* (1987) also found some indication that part of the vacancies could be on A sites as well.

The magnetic structure of γ-Fe_2O_3 basically consists of an alternation of two opposed but unequal magnetic sublattices, i.e. the ferrimagnetic structure (Néel 1948). The atomic Fe^{3+} moments within each sublattice are coupled parallel, whereas those of the A and B sublattices are coupled antiparallel through an intervening O^{2-} anion. Because of the non-equivalence of the sublattice magnetizations, a strong net ferrimagnetic moment results in maghemite. For the most common maghemite varieties with only octahedral vacancies, an average excess of $\frac{1}{2}Fe^{3+}$ exists on the B sublattice per formula unit (pfu) γ-Fe_2O_3. This corresponds to a net magnetic moment pfu of 2.5 μ_B, implying a theoretical saturation magnetization of $\approx 87\ Am^2\ kg^{-1}$, at 0 K with zero thermal energy. A typical room temperature value of $74\ Am^2\ kg^{-1}$ is often found for this maghemite type (e.g. Johnson & Merrill 1974; Bate 1980; Goss 1988; Özdemir & Dunlop 1988; Özdemir 1990; Moskowitz 1993). The presence of part of the vacancies on tetrahedral interstices would result in a higher net magnetic moment. Takei & Chiba (1966) obtained a net magnetic moment pfu Fe_2O_3 of 2.9 μ_B for their synthetic maghemite variety, which would imply that nearly 20 per cent of the total amount of vacancies would occupy tetrahedral interstices.

Direct measurement of the Curie point of pure maghemite is often not possible, because of its inversion to haematite at lower temperatures, i.e. $T_{inv} < T_C$. Determination of T_C by indirect methods or by calculations yielded values between ≈ 590 and 770 °C (e.g. Michel & Chaudron 1935; Maxwell *et al.* 1949; Aharoni *et al.* 1962; Frölich & Vollstädt 1967; O'Reilly 1968; Readman & O'Reilly 1972; Da Costa *et al.* 1995). The few direct measurements reported in the literature indicate a T_C of around 640–645 °C for tetragonally ordered γ-Fe_2O_3 (Özdemir & Banerjee 1984; Heider & Dunlop 1987; Van Oorschot & Dekkers 1999). However, the effect of different ordering of vacancies or cations over the two magnetic sublattices is not yet known exactly. Takei & Chiba (1966), for instance, measured a T_C of 470 °C for their pure maghemite with tetrahedral vacancies.

2.3 Crystallographic relations between γ-Fe_2O_3 and α-Fe_2O_3

The transformation of γ-Fe_2O_3 to α-Fe_2O_3 is considered to be topotactic, occurring by restacking of close-packed oxygen ion layers (ccp to hcp) accompanied by displacement of interstitial ferric ions rather than by wholesale recrystallization (e.g. Bernal *et al.* 1957, 1959; Kachi *et al.* 1963). Plate-like haematite crystals grow with their (0001) planes in the (111) planes of

the maghemite, and with the [111] and [110] axes of maghemite corresponding to the [0001] and [100] axes of haematite, respectively (*cf.* Cornell & Schwertmann 1996).

3 SAMPLES AND EQUIPMENT

3.1 Samples

Six natural haematites and three synthetic samples prepared according to different recipes were used. The natural samples were upgraded from various raw haematite ores or macroscopic haematite crystals (museum pieces). Previous rock-magnetic studies on this material include those of Dankers (1978, 1981), who studied the haematite samples labelled LH2 (Kimberley, South Africa) and LH3 (Framont, France). Hartstra (1982) investigated samples LH4 (origin unknown), LH6 (Gellivara, Lapland) and LHC (origin unknown). The haematite material from the Kadan locality in the Czech republic was previously studied by Hejda *et al.* (1992) and Petrovský *et al.* (1994, 1996). The low-temperature behaviour of these natural samples was described in De Boer (1999). Table 1 shows the chemical composition of the haematites determined by microprobe analysis; no significant isomorphous substitution was detected.

For our investigations, we used the mineral concentrates made by Dankers and Hartstra, whereas new grain-size fractions of the Kadan haematite were prepared. The high-purity haematite concentrates of Dankers and Hartstra were separated by a procedure which briefly comprised of crushing the raw ore in a copper mortar followed by further separation according to haematite's specific density and magnetic properties by means of a heavy liquid overflow-centrifuge and a Frantz isodynamic magnetic separator, respectively. We obtained sized fractions of the Kadan haematite by crushing crystal fragments in a copper mortar followed by sieving. The fragments were cut from macroscopic acicular crystals ($\sim$10 cm long) using a small diamond drill. Only fresh, pure haematite from the inner parts of the needles was selected. With the exception of traces of quartz, no minerals other than haematite were detected in the mineral concentrates using X-ray diffraction analysis and optical microscopy. Examples of X-ray diffraction analyses are shown in Figs 3(a) and (c) for Kadan and LH3 haematite, respectively.

The first type of synthetic haematite samples were prepared by transformation of (2-line) ferrihydrite in aqueous solution according to the procedure described by Schwertmann & Cornell (1991; Method 4). In brief, several well-cleaned glass bottles filled with $\approx$250 mL of a 0.1 molar ferric nitrate solution were heated at 97 °C for 48 hr in a water bath. In this way haematite is precipitated via intermediate ferrihydrite, that is, a poorly ordered iron oxyhydroxide. After termination of the synthesis the samples were washed salt-free, centrifuged and the excess solution was removed before the material was dried in a stove for 1 day at approximately 40 °C. A sample, previously made ($\approx$1 yr before) under identical conditions by Thomas Pick and stored in the mother solution, was also available for thermomagnetic analysis. The synthesis product is a dark reddish-brown powder consisting primarily of haematite, although some goethite and ferrihydrite traces are usually present. The major part of the haematite occurs in anhedral crystals smaller than $\sim$0.1 μm, although some coarser (0.1–10 μm) hexagonal crystals may also be present (*cf.* Schwertmann & Cornell 1991). Stocking & Tauxe (1990) synthesized α-Fe_2O_3 under similar conditions and described similar features of the haematite.

The second haematite type was prepared by dehydration of synthetic goethite. The goethite was prepared from analytical grade iron(III)-nitrate [$Fe(NO_3)_3 \cdot 9H_2O$] and described by Dekkers & Rochette (1992). Dehydroxylation ($\approx$35 mg) was carried out in air in the open-ended furnace of the Curie balance by repeated heating and cooling cycles to increasingly higher temperatures using heating and cooling rates between 1 and 10 °C min^{-1}. In this way, the thermal decomposition of the goethite could be followed and the creation of a possible ferrimagnetic phase could be detected instantly.

The third synthetic haematite samples were prepared by heating analytical grade iron(III)-nitrate to 800 °C in a Curie balance and also in a bigger furnace, using $\approx$50 mg and 10 g starting material, respectively. The synthesis in the Curie balance was either achieved by one thermal cycle to 800 °C or by repeated cycles to increasingly higher temperatures using heating and cooling rates of 10 °C min^{-1}. In the bigger furnace, the Fe-nitrate salt was heated with 10 °C min^{-1} to $\approx$350 °C. The sample was held at this temperature for almost 30 min. During this time the furnace was opened to allow the yellowish-brown gas (NO_2) to escape. Some amount of the brownish-red material formed was sampled before the other portion was heated to 800 °C. Every 100° the furnace was opened for a short period, allowing the freshly produced gas to escape. Cooling was achieved by just opening the furnace. The material obtained consists of fine-grained ($<$1 μm) dark-red particles and some grey-coloured clusters of fused haematite particles. Nininger & Schroeer (1978) also prepared haematite by thermal decomposition of ferric-nitrate salts. They found that the size of the particles was dependent on both the temperature and the duration of the heating. They obtained a particle size of 500 ± 30 Å for a sample heated at 347 °C for 30 min. The low-temperature behaviour of the α-Fe_2O_3 heated to 800 °C in the big furnace was described in De Boer (1999).

Table 1. Chemical composition of the natural haematite samples used in this study as determined by (1) Dankers (1978, 1981), (2) Hartstra (1982) and (3) Hejda *et al.* (1992) using microprobe analysis.

	LH2 (1)	LH3 (1)	LH4 (2)	LH6 (2)	LHC (2)	Kadan (3)
Fe_2O_3 (%)	98.2	98.2	97.9	98.1	99.9	$\sim$99
Al_2O_3 (%)	0.1	0.3	0.6	0.7	0.5	$<$0.1
TiO_2 (%)	$<$d.l.	$<$d.l.	0.1	0.5	$<$d.l.	$<$0.1
Cr_2O_3 (%)	$<$d.l.	$<$d.l.	0.3	0.2	$<$d.l.	$<$0.1
SiO_2 (%)	0.4	0.4	0.9	$<$d.l.	0.1	$<$0.1
V_2O_3 (%)	nd	nd	0.7	0.5	$<$d.l.	$<$0.1
MnO (%)	$<$d.l.	$<$d.l.	0.1	0.2	0.1	$<$0.1
MgO (%)	$<$d.l.	$<$d.l.	nd	nd	nd	$<$0.1

$<$d.l., lower than detection limit; nd, not determined.

3.2 Equipment used

Thermomagnetic analyses were performed in air using a modified horizontal translation Curie balance that makes use of a cycling field (Mullender *et al.* 1993). Previous measurements showed that the atmosphere inside the open-ended furnace unit stays oxidizing up to the highest possible temperature of 800 °C. Step-scanned X-ray diffractograms (0.02°2Θ, counting time 1 s) were recorded with a Philips PW 1700 diffractometer using Cu–K_α radiation and silicon as internal standard.

Thermogravimetric analysis, a method that measures the mass change of a sample on heating with a specified rate, was performed in air. A Princeton alternating gradient magnetometer (MicroMag 2900) equipped with a helium flow-through cryostat was used to monitor low-temperature (room temperature to -230 °C) cooling and warming runs of induced remanence (2 T), and to measure hysteresis loops at room temperature. Cooling and warming rates were ~ 5 °C min^{-1}.

4 EXPERIMENTAL RESULTS AND DISCUSSION

4.1 Natural haematite samples

4.1.1 Thermomagnetic analyses

Figs 1(a)–(f) show the thermomagnetic behaviour of various natural haematites. The four uppermost panels (a–d) illustrate behaviour commonly encountered for pure haematite. Samples LHC, LH2 and LH6 show behaviour characteristic of non-saturated, pure defect-poor haematite magnetically dominated by the canted moment (*cf.* De Boer & Dekkers 1998). The gradual increase in magnetization observed during initial heating is caused by the decrease in coercivity allowing an increasing portion of the magnetic domains to become aligned with the field. Heating above the Curie point (700 °C cycle) results in the typical irreversible block-shaped cooling curve whose shape only depends on the temperature variation of the exchange energy. Heating to 800 °C slightly improves the crystallinity, as can be deduced from the small gain in magnetization compared to that after the 700 °C cycle, but no creation of an additional magnetic phase is observed. The behaviour shown by LH4 haematite (Fig. 1c) is characteristic of α-Fe_2O_3 rich in structural defects (*cf.* De Boer & Dekkers 1998). On heating to 800 °C the defects are progressively annealed out of the lattice resulting in the block-shaped curve typical of defect-poor haematite. The removal of this specific type of internal defect obviously does not trigger the formation of a new magnetic phase. The break in slope at ≈ 100 °C is interpreted as the high-temperature onset of the Morin transition.

In contrast, Figs 1(e) and (f) show thermomagnetic behaviour noticeably different from that described above. Both figures illustrate that the formation of a magnetic phase from haematite on heating is possible. At first, until cycling to ≈ 700 °C, Kadan and LH3 haematite show thermomagnetic behaviour similar to that observed for non-saturated, defect-poor haematite. Mass-specific magnetization values and Curie temperatures are typical of pure haematite. For Kadan haematite, the small tail of increasing magnetization observed at the end of the cooling curve of the 700 °C cycle, however, is a first indication for the development of a new magnetic phase, although a distinct Curie temperature is not yet visible. On cooling from 800 °C, the thermomagnetic curves of both samples, however, clearly reveal the presence of an additional magnetic phase which is characterized by a magnetic ordering temperature of ≈ 470–475 °C. No noticeable shift in Curie temperature of the haematite phase itself is observed.

For sample LH3, the part of the cooling curve representing the new magnetic phase is identical in shape to that usually observed for ferrimagnetic magnetite and maghemite. Furthermore, its specific shape suggests that the major part of the grain sizes of the new phase lie above the single-domain (SD) threshold size, whereas the exponential shape observed for the Kadan sample suggests a high contribution of ultra-fine superparamagnetic (SP) particles. In addition, the differences in mass specific magnetization obtained after the 800 °C cycle indicate that a considerably higher amount of the new magnetic phase is created from platy-developed LH3 haematite than from acicular Kadan haematite particles that are elongated in the *c*-direction. These findings suggest that the new magnetic phase could be an epitaxial(?) spinel outgrowth that may have some relation to prevalent haematite crystal faces. No magnetic phase is created from relatively large uncrushed ore chips of Kadan haematite treated under identical conditions (*cf.* Petrovský *et al.* 1996). This could also be interpreted as there simply being no appropriate crystal planes available to grow the spinel phase on.

4.1.2 MicroMag measurements

The Kadan sample was heated to temperatures above 800 °C in a furnace different from the Curie balance, first to investigate its thermal stability and second possibly to get a higher yield of the new magnetic phase necessary for a proper X-ray diffraction analysis. In this closed furnace, heating rates were similar to those in the Curie balance but cooling was carried out in an uncontrolled way by turning off the power supply. Cooling to room temperature commonly lasted for ≈ 12 hr. The results of these heatings are shown in Fig. 2, together with additional magnetic measurements of the original material and material heated in the furnace at 600 °C.

The hysteresis loop obtained for the original Kadan haematite is typical of a high-coercivity mineral. No trace of a low-coercivity mineral was detected in this sample. The hysteresis loops measured on the heated material, however, clearly demonstrate the progressive development of a low-coercivity phase from the haematite sample with increasing temperature, that is, the loops become increasingly wasp-waisted. The first traces of the new magnetic phase are now already detected after heating to 600 °C, probably because of the longer exposure to this temperature compared to the Curie balance measurements. The magnetic characteristics of the material being heated to temperatures above 800 °C show not only that the new magnetic phase is persistent to these high temperatures but also that the formation process was not yet fully completed. Furthermore, the progressive change in shape of the thermomagnetic curves from concave for the material preheated at 600–900 °C to convex for the material preheated at 1000 °C, indicate an increase in grain size of the new magnetic phase. After the heating at 1000 °C, almost all of the material was attracted to a hand magnet, indicating that this is most likely intergrown material, possibly epitaxial outgrowths of the magnetic phase on the haematite parent, rather than with some isolated contamination.

4.1.3 X-ray diffraction analysis

The X-ray diffraction patterns obtained for the original Kadan (Fig. 3a) and LH3 (Fig. 3c) samples show, besides strong haematite reflections, only some minor peaks revealing the presence of traces of quartz. No other impurities were recognized. For both samples, the positions of the haematite peaks and their relative intensities concur well with those reported for pure α-Fe_2O_3. The diffractograms of heated Kadan

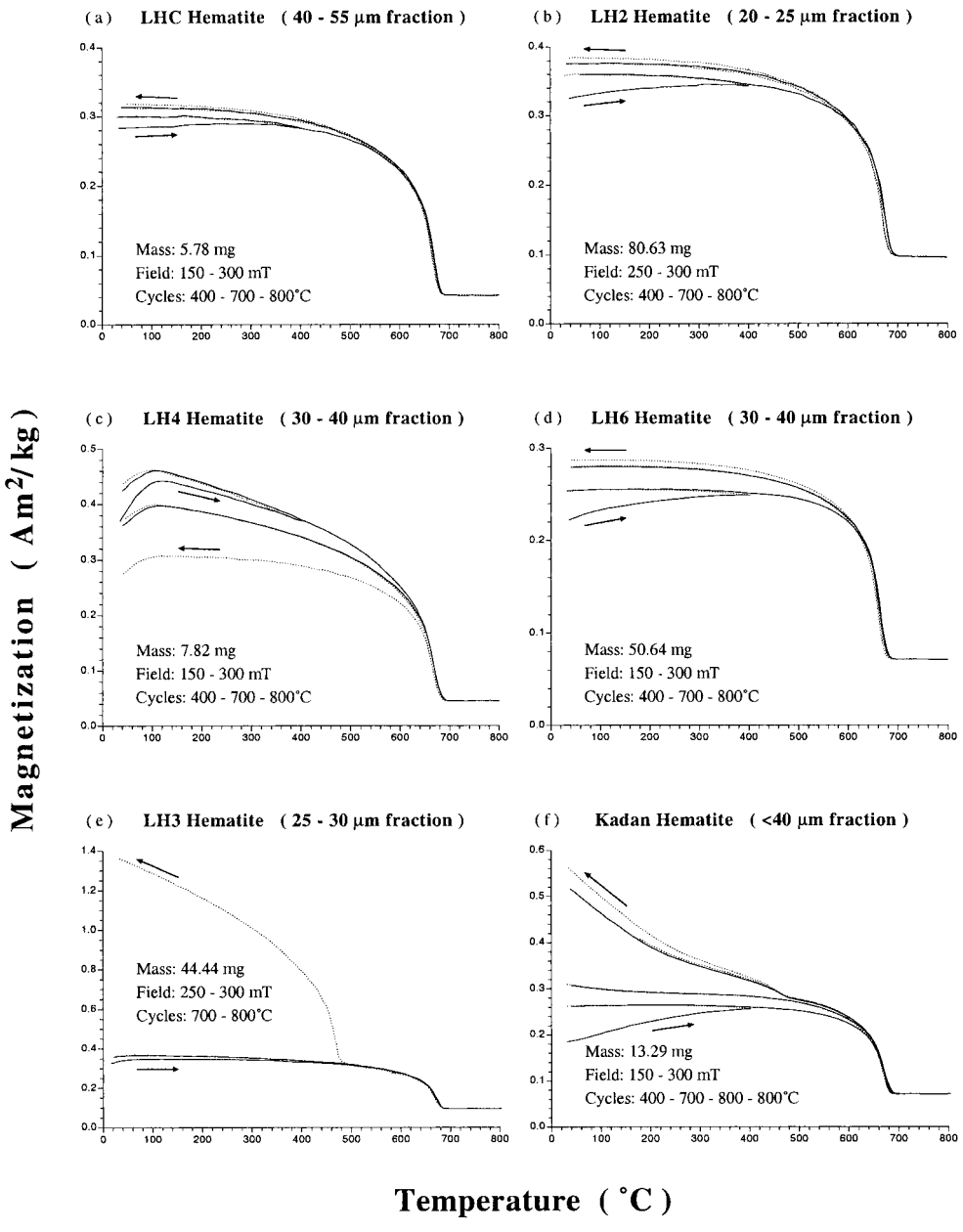

Figure 1. Thermomagnetic behaviour of various natural haematite samples. Solid and dotted lines denote heating and cooling curves, respectively. Panels (a) (b) and (d) illustrate thermomagnetic behaviour typical of non-saturated defect-poor haematite, magnetically dominated by the canted moment, whereas the behaviour shown in panel (c) is characteristic of a more defect-rich haematite whose defect moment becomes progressively reduced on heating. The specific break in slope at ≈ 100 °C represents the high-temperature onset of the Morin transition. Panels (e) and (f) show the formation of traces of a new magnetic phase from haematite after heating to ≈ 700–800 °C. This new magnetic phase is characterized by a Curie temperature of ≈ 470–475 °C.

(Fig. 3b) and LH3 (Fig. 3d) samples clearly reveal additional reflections characteristic of a cubic spinel phase. The high relative intensities of the peaks representing the (111), (222) and (333) planes again suggest that the spinel phase has a distinct crystallographic relation to the parent haematite. Cubic unit cell dimensions found for the spinel phase grown on Kadan and LH3 haematite are both $a_0 = 0.8350 \pm 0.0005$ nm. This value falls in the range commonly reported for pure maghemite, and it is also similar to the cell dimension of the maghemite described by Takei & Chiba (1966). On the other hand, the same unit cell length will be obtained for a magnetite substituted with a certain amount of an ion smaller in size than the iron ion, such as, for instance, Al^{3+} (e.g. Schwertmann & Murad 1990), something we regard as unlikely. No shift in the positions of the X-ray diffraction peaks belonging to haematite is observed after heating.

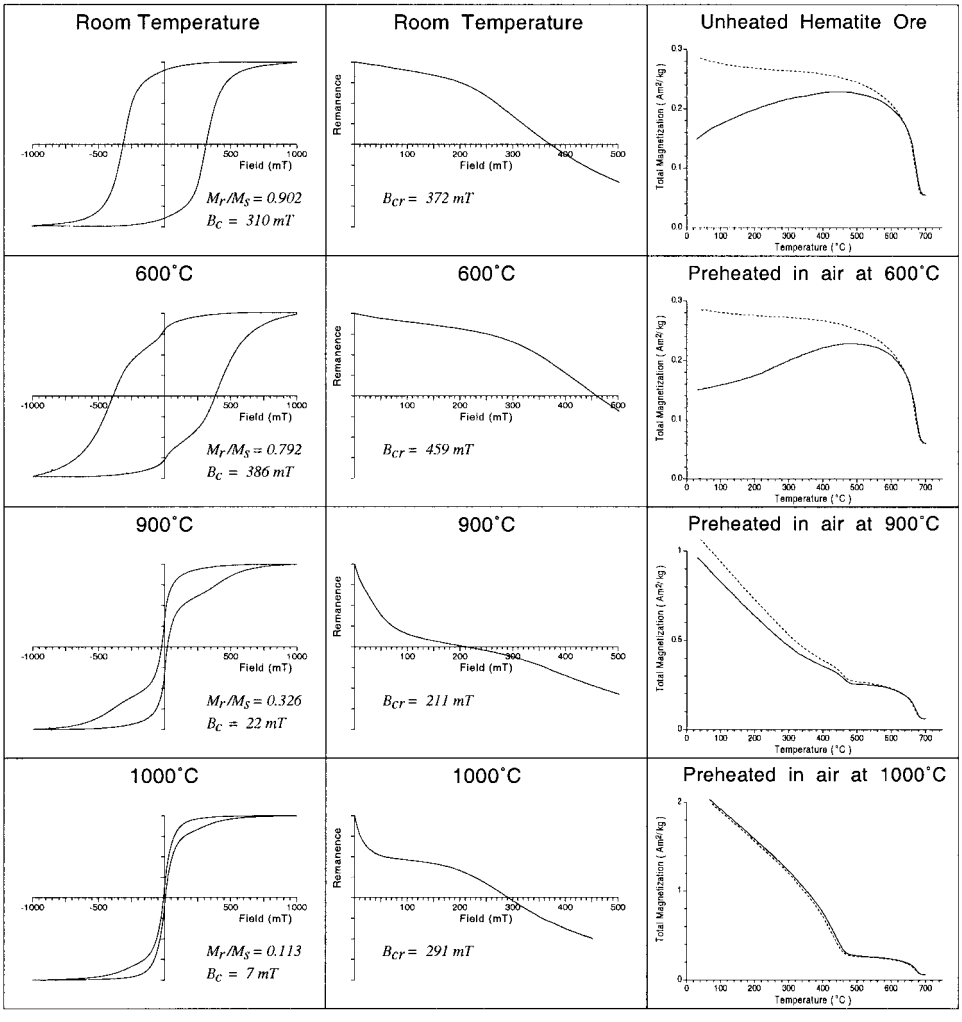

Figure 2. MicroMag measurements at room temperature and thermomagnetic analysis of original Kadan haematite and samples heated in a furnace to 600, 900 and 1000 °C, clearly showing the progressive development of a highly magnetic low-coercivity phase from pure haematite with increasing temperature. Hysteresis loops are slope corrected.

4.1.4 Low-temperature behaviour of imparted remanence

Fig. 4 shows a low-temperature cycle, between 0 and −230 °C, of imparted remanence (2 T) for sample LH3 preheated in a Curie balance to 800 °C. After cooling to *c.* −50 °C, that is, below the Morin transition of haematite, ≈85 per cent of the initial remanence still remains. This indicates that, as suggested earlier, at least part of the spinel phase particles are larger in size than the SP threshold size of ≈25–30 nm. On further cooling, hardly any change in remanence is observed, whereas on warming back to room temperature a gradual decrease in intensity occurs until ≈75 per cent of the initial IRM. No indication of a Verwey transition is observed, which excludes the possibility that the spinel phase is a slightly substituted or slightly oxidized magnetite. On the other hand, the specific behaviour observed concurs well with the behaviour described earlier for maghemite by Dankers (1978) and De Boer & Dekkers (1996).

4.2 Synthetic haematite samples

4.2.1 Fe(III)nitrate and ferrihydrite precursors

Figs 5 (a) and (b) show the thermomagnetic behaviour of synthetic haematite samples prepared from a hydrated ferric nitrate precursor and (c) and (d) show a ferrihydrite precursor. Evidently, a magnetic spinel phase with $T_c \approx 470$–475 °C, similar to the one described earlier for the natural haematite samples can be created from both synthetic haematites (a) and (d) on thermal cycling. The conditions during and after the formation of the haematite phase, however, seem to be a crucial factor determining whether the additional magnetic phase is created on heating or not. The thermal decomposition of highly pure $Fe(NO_3)_3 \cdot 9H_2O$ to haematite is monitored during a standard thermomagnetic analysis in a Curie balance using heating and cooling rates of 10 °C min^{-1} (Fig. 5a). The initial decrease in magnetization on heating agrees reasonably

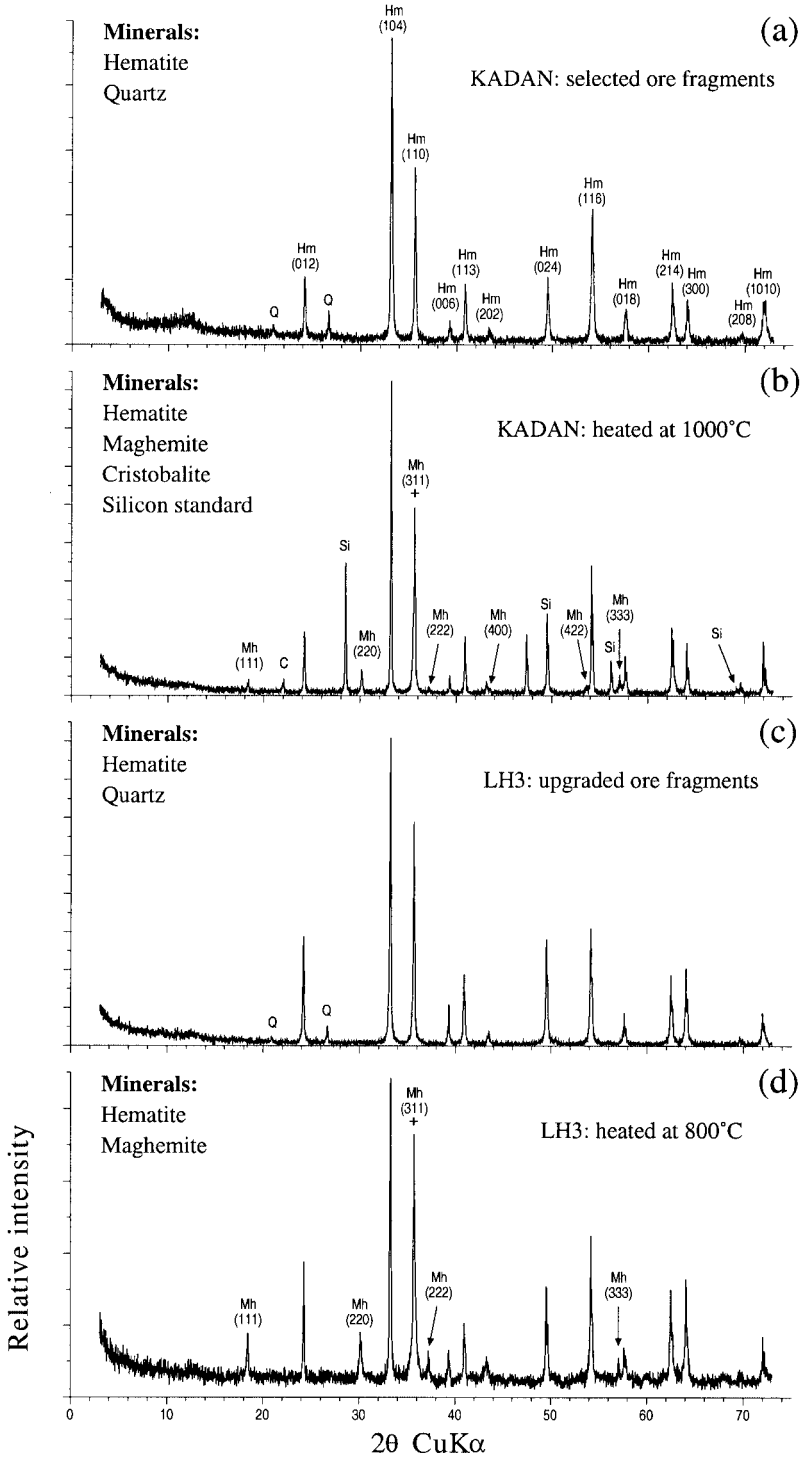

Figure 3. X-ray diffraction patterns of (a) original Kadan haematite and (c) original LH3 haematite and after heating the material to (b) 1000 °C and (d) 800 °C (magnetic concentrate), respectively. The heated samples clearly show additional peaks belonging to the cubic spinel structure of maghemite. Reflections of haematite, maghemite, quartz, cristobalite and the silicon standard are denoted by Hm, Mh, Q, C and Si, respectively.

well with reported melting and decomposing points of the monoclinic nitrate salt, being 47.2 and 125 °C, respectively (CRC Handbook of Chemistry and Physics). Obviously, an appropriate haematite type necessary to create the magnetic phase can be formed when applying one single heating cycle between room temperature and ~750 °C (Fig. 5a). Subsequent heating to 800 °C and annealing for 30 min (not shown here) causes almost reversible thermomagnetic behaviour, indicating that the maghemite-like phase is persistent to this high temperature and that no additional amount was formed.

On the other hand, stepwise cycling to increasingly higher temperatures (not shown here) or keeping the sample for a certain time at an intermediate temperature (e.g. 200 or 350 °C) before further heating to 750 or 800 °C does not favour the

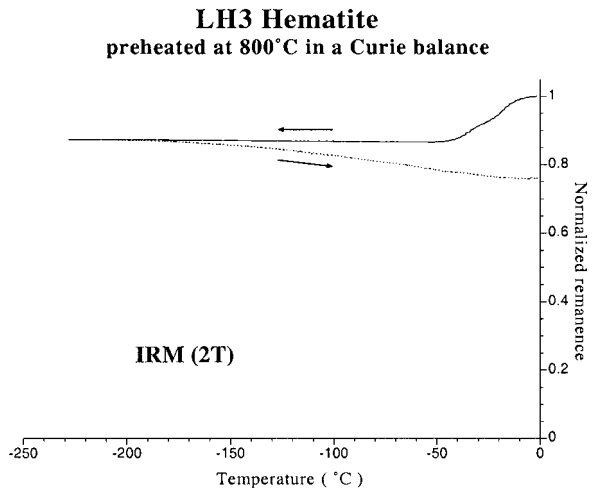

Figure 4. Low-temperature cycling of a 2 T IRM imparted at room temperature for sample LH3 after a thermal cycle to 800 °C in a Curie balance.

formation of the haematite type required, that is, no additional magnetic phase is created on heating. Fig. 5(b), for instance, shows the thermomagnetic analysis of a haematite sample produced by heating the nitrate salt to 350 °C in a furnace and keeping the sample at this temperature for half an hour before heating to 800 °C where it was annealed for 1 hr.

When dealing with a Fe(III)nitrate precursor, the specific thermal cycling procedure used thus seems to determine whether the appropriate haematite type is actually formed that is required to create the maghemite-like phase on (further) heating. Again, these observations do not support any suggestion that the spinel phase is created by diffusion of impurity cations towards the surface, because this process is probably not dependent on the heating procedure used, but rather on the height of the temperature reached and holding time at the annealing temperature. Cations incompatible with the haematite structure will be expelled from the crystal lattice irrespective of the heating procedure. If the formation of the maghemite-like phase was related to those impurities, it would always form, which is in contrast to the observations. Consequently, the formation of

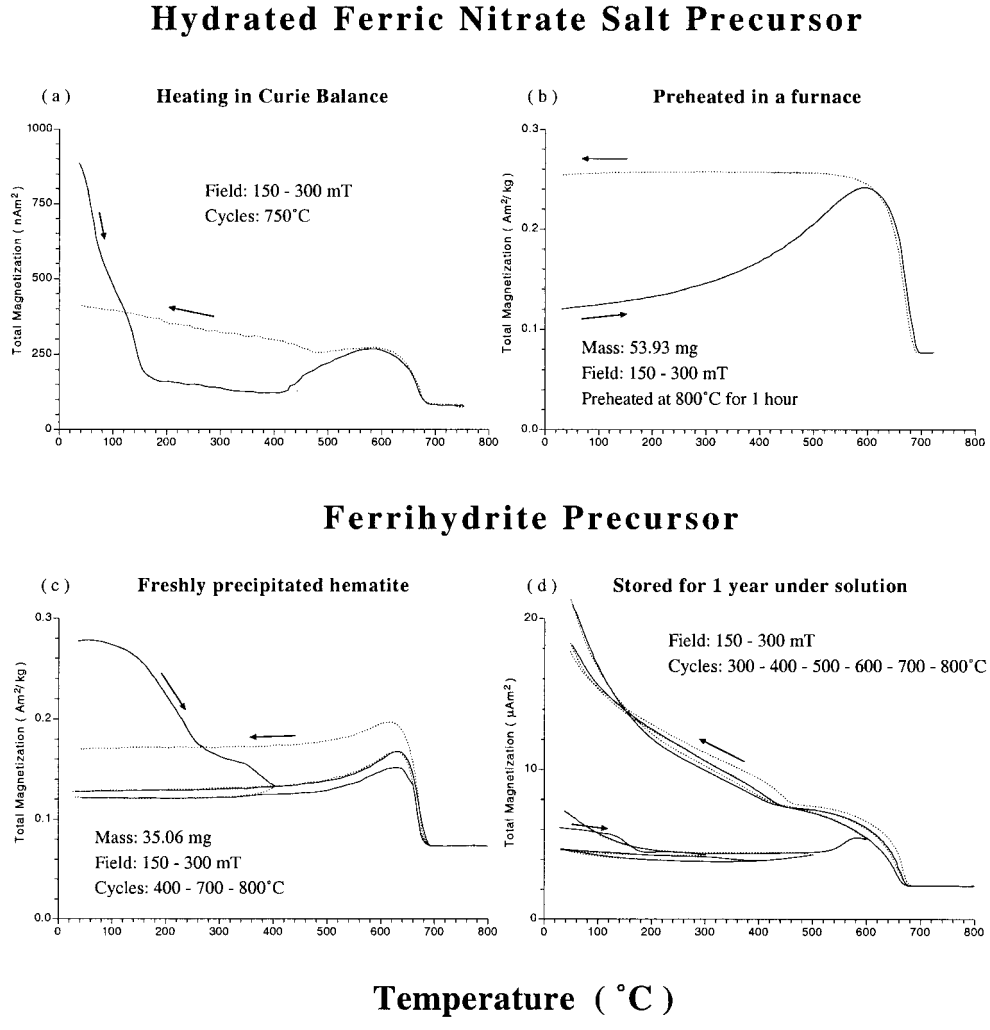

Figure 5. Thermomagnetic behaviour of synthetic haematites prepared from different precursor minerals. Panel (a) shows the thermal decomposition of a hydrated ferric nitrate salt to haematite and the subsequent formation of an additional magnetic phase with a T_c of $\approx$470 °C. Panel (b) shows a thermomagnetic analysis of a haematite sample prepared from the same starting material which was preheated to 800 °C in a furnace with a 30 min intermediate heating step at 350 °C. (c) Thermomagnetic behaviour of a synthetic haematite freshly precipitated from a ferric nitrate solution via a ferrihydrite stage. (d) Haematite sample synthesized under identical conditions to (c) after $\approx$1 yr storage in the mother solution.

the spinel phase must rather be associated with another type of internal defects of which the concentration varies with the preparation method.

Figs 5(c) and (d) show the thermomagnetic analysis of a haematite sample freshly precipitated from an iron nitrate solution via an intermediate ferrihydrite stage and a sample synthesized under identical conditions, left for almost 1 yr in the mother solution, respectively. A magnetic phase with a Curie temperature of 470–475 °C is created only from the second sample during thermal cycling. The first appearance of the maghemite-like phase can already be deduced from the tail of increasing magnetization after the 400 °C cycle. A distinct Curie point, however, can only be recognized after the 600 °C cycle. The spinel phase does not survive annealing at 1000 °C (not shown here).

The initial two-step decrease in magnetization observed for both samples is probably due to a goethite and a ferrihydrite impurity, each with a different dehydration temperature trajectory. Because both samples show this initial behaviour it is not likely that these impurities are responsible for the creation of the highly magnetic phase. Also, note that the natural haematite samples described earlier did not have these contaminations. Consequently, changes in the precipitated haematite during storage must thus be responsible for the different thermomagnetic behaviour. The thermomagnetic behaviour representative of the haematite phase gives several clues for these changes. The Hopkinson-like peak in magnetization lies at a lower temperature for the stored sample and it shows a block-shaped cooling curve after heating above the Curie point, whereas the cooling curve of the freshly precipitated sample still shows the Hopkinson-like peak. According to De Boer & Dekkers (1998), both observations probably indicate that the stored sample is magnetically slightly softer, in this case presumably caused by an improved crystallinity and/or an increase in grain size. The process of Ostwald ripening—the growth of large particles in a suspension at the expense of the smaller ones which redisolve—may be put forward as a cause for this magnetic observation. In addition, less stable phases such as ferrihydrite will convert to more stable haematite, which explains the lower contribution to the signal of these impurity minerals for the stored sample.

4.2.2 *Goethite precursor*

Figs 6(a)–(c) show the changes in magnetization during the thermal decomposition of a synthetic goethite to haematite and the subsequent heating-induced crystal structure improvement and grain-size increase. The thermomagnetic behaviour of this synthetic goethite is described in De Boer & Dekkers (1998) for cycling up to 100 °C. Subsequent cycling to 150 and 200 °C slightly alters the goethite phase, as can be deduced from the irreversibility of the curves (that is, decrease in magnetization) and the shift of the Hopkinson-like peak to higher temperatures. The latter also indicates that the magnetic hardness of the goethite increases. On further cycling, the distinct drop in magnetization between 200 and 250 °C marks the major dehydroxylation step of the goethite phase to haematite. During the 400 °C cycle, the transformation to haematite is completed. Using this technique, no indication for the existence of a spinel phase is found. Other authors (e.g. Özdemir 1998), however, have reported the possible formation of intermediate magnetite during the transformation reaction.

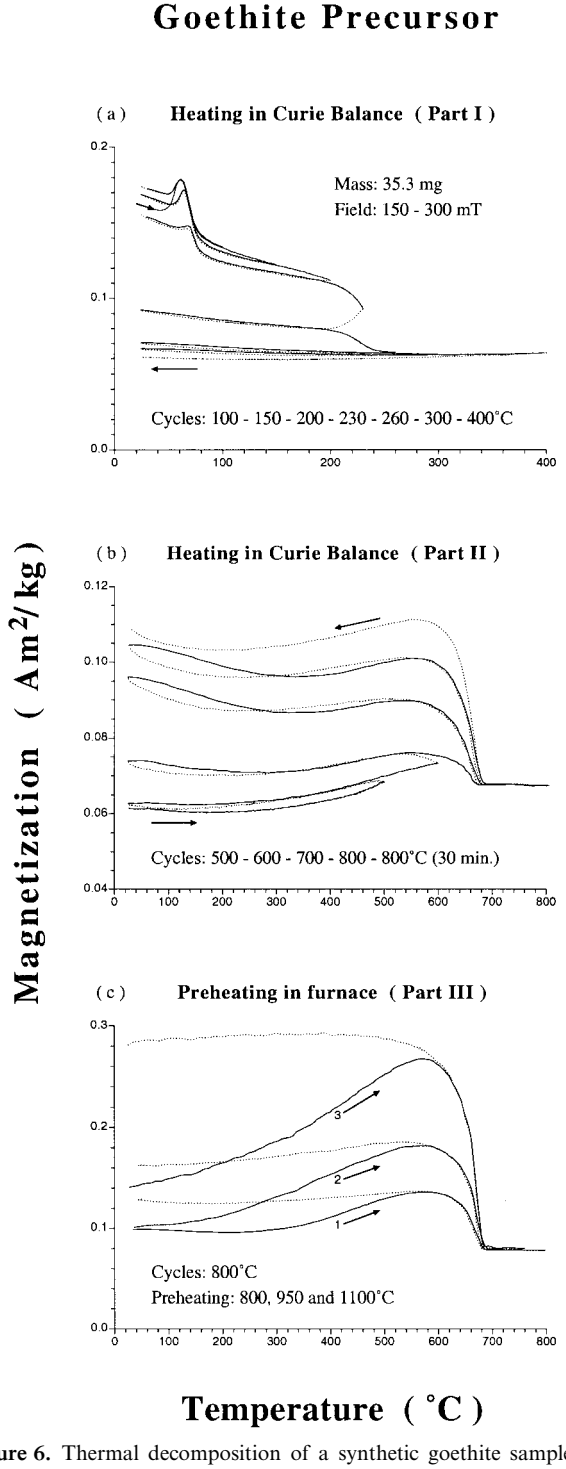

Figure 6. Thermal decomposition of a synthetic goethite sample as observed in a Curie balance during repeated runs to increasingly higher temperatures. Panel (a) shows the dehydroxylation to poorly ordered fine-grained haematite, whereas panel (b) illustrates the subsequent heating-induced crystallinity improvement and crystallite growth. The exponential tail in the magnetization curves observed at their low temperature side most probably represent the ultrafine-grained part of the haematite crystallites becoming SP on heating, rather than it indicating the possible existence of traces of an additional magnetic phase. Panel (c) shows the thermomagnetic behaviour of the sample after annealing in a furnace for several hours at 800 °C (1), 950 °C (2) and 1100 °C (3). Annealing at 1100 °C resulted in a perfectly ordered defect-poor haematite whose thermomagnetic behaviour is similar to that observed for the natural samples in Figs 1(a), (b) and (d).

Haematite formed in this way is reported (e.g. Chevallier 1951) to be extremely fine grained and is generally superparamagnetic, i.e. <0.03 μm. The α-Fe_2O_3 particles just above the SP threshold size appear to be extremely hard (e.g. Dekkers 1990), implying that they are far from being saturated in the magnetic fields possible in the Curie balance. The progressive gain in magnetization on repeated cycling to increasingly higher temperatures (Fig. 6b) shows that the particles become magnetically increasingly softer. This illustrates the continued heating-induced growth of the haematite crystallites. Obviously, during this process, no spinel phase with a distinct Curie point is created on the α-Fe_2O_3 particles. Although the typical tail in magnetization at the low-temperature side of the curves may indicate the presence of ultrafine-grained spinel particles, it is more likely to be explained by very small SD haematite particles which become SP on mild heating (<300 °C). The temperature hysteresis between a cooling curve and the heating curve of the subsequent cycle may represent some sort of hard VTRM. This behaviour resides up to 950 °C (Fig. 6c). Only after annealing at 1100 °C does the sample show a block-shaped cooling curve characteristic of well-ordered defect-poor haematite.

4.3 Possible formation mechanism of the spinel phase

The observed behaviour may represent the crystallographic $\alpha \rightarrow \gamma$ transformation described by Finch & Sinha (1957). Meillon *et al*. (1995) also conclude that this transformation can occur under appropriate conditions. The Curie point of the new phase, however, does not concur with T_c ($\approx$640–645 °C) reported for the most common maghemite type with octahedrally coordinated vacancies only. On the other hand, it is identical to the T_c reported by Takei & Chiba (1966) for an epitaxially grown maghemite type with a suggested portion ($\approx$20 per cent) of its vacancies on tetrahedral interstices. Before accepting this option, two aspects need to be explored further: (i) an independent observation substantiating the surficial character of the maghemite; and (ii) other possibilities to obtain a Curie point of 470 °C.

The behaviour observed during citrate–bicarbonate–dithionite extraction according to the procedure described by Van Oorschot & Dekkers (1999) supports the surficial character of the maghemite impurity. Stepwise extraction of $\approx$100 mg Kadan grains (<40 μm) was carried out at 60 °C (45 ml extraction solution, 1 g dithionite added per step, no matrix present). After the first step, low-field susceptibility was $\approx$40 per cent of the starting value and after a second step $\approx$3.5 per cent, while thermomagnetic runs (not shown here) still recorded the Curie point of 470 °C. These findings show that the maghemite is not contained inside the haematite grains because then it would not be attacked by the reductive dissolution. The observed dissolution behaviour is fully compatible with fine-grained material.

Other possibilities to explain the T_c found would be the presence of newly formed varieties of substituted magnetite or maghemite. If these phases are formed from haematite, this would imply that certain foreign cations present in the haematite structure become incompatible on heating and are expelled from the lattice forming a spinel surface layer rich in these elements. Following the molecular-field approximation for ferrimagnetism, most impurity cations in the spinel lattice will cause a more or less linear decrease in T_c with increasing substitution. To get a T_c of 470 °C, for instance, magnetite must be substituted with $\approx$20 mole per cent Ti (e.g. Readman & O'Reilly 1972). For maghemite, a substitution of $\approx$50 per cent Ti (e.g. Readman & O'Reilly 1972) or $\approx$20 per cent Al (e.g. Da Costa *et al*. 1995) is required. Other spinel phases with reported Curie points in the mentioned temperature range are $CoFe_2O_4$ (520 °C), $CuFe_2O_4$ (455 °C), $MgFe_2O_4$ (440 °C) and $MnFe_2O_4$ (300 °C) (e.g. Smit & Wijn 1959). In this view, however, it is remarkable that the other haematite types with similar or even higher traces of foreign cations in their lattices do not show comparable behaviour. Moreover, it would be highly coincident that from both haematites a substituted spinel is created with exactly the same Curie point.

The low Curie point of $\approx$470 °C, however, indicates that the super-exchange bonds existing in the specific maghemite created during our experiments must be less in amount or less strong compared to the bonds present in the most common maghemite varieties with all vacancies on octahedral sites and a characteristic T_c at $\approx$645 °C. The difference may be explained by an odd arrangement of the vacancies and/or cations over the octahedral and tetrahedral sites. The epitaxially grown maghemite variety described by Takei & Chiba (1966), for instance, has an identical T_c of 470 °C. Various analyses performed by these authors clearly showed that it was a pure ferric oxide form, discounting the possibility that any impurity cation was responsible for the lowering of the T_c. Moreover, their measured value for the first cubic magnetocrystalline anisotropy constant K_1 of -4.6×10^3 J m^{-3} agrees closely with the value $K_1 = -4.7 \times 10^3$ J m^{-3} calculated by Birks (1950), based on measurements of initial permeability for polycrystalline maghemite (*cf.* Dunlop & Özdemir 1997). Combining our findings with the results of Finch & Sinha (1957) and Takei & Chiba (1966) seems to suggest that the arrangement of vacancies and/or cations in outgrowings of maghemite on certain specific substrates can be different from that usually encountered in distinct maghemite particles. The structure suggested by Takei & Chiba (1966), with approximately 20 per cent of the vacancies on tetrahedral sites, may also be adopted in our case, especially when one takes into consideration that all Fe^{3+} ions in the haematite parent are octahedrally coordinated.

The fact that the α-$Fe_2O_3 \rightarrow \gamma$-$Fe_2O_3$ transformation takes place at the surface of the haematite particles strongly suggests that, in our case, a thermally activated outward migration of some specific type of internal defects forces the necessary structural rearrangement from a thermodynamically stable hcp to a less stable ccp stacking of the oxygen layers. The thermomagnetic behaviour of sample LH4, however, shows that not every type of internal defect can trigger this process because no spinel is created on heating. The haematites from which the spinel phase is created must thus have a specific type of defect in common. These defects must be present in sufficient concentration and presumably migrate to grain edges on heating.

In general, the type and concentration of internal defects is highly determined by the mode of formation. It is known from the literature that most haematites produced in aqueous systems or by thermal dehydration of either hydrated nitrate salts or goethite often retain some incorporated hydroxyl groups in the structure (e.g. Gallagher & Gyorgy 1969; Wolska 1981; Šubrt *et al*. 1984; Wolska & Schwertmann 1989; Schwertmann & Cornell 1991; Waychunas 1991; Stanjek & Schwertmann 1992). The hydroxyl groups replace O^{2-}

anions in the haematite crystal lattice (Wolska 1981; Wolska & Schwertmann 1989). The electroneutrality is preserved by Fe^{3+} deficiency in the cationic positions, rather than by changing the valence state of some Fe^{3+} to Fe^{2+}. Moreover, Wolska & Schwertmann (1989) showed that these hydroxyl groups can be extremely persistent against heating. Complete removal may require temperatures up to *c.* 1000 °C. Their release on heating implies some rearrangement of the haematite structure. When present in appropriate concentrations this process may possibly trigger the formation of the maghemite-like phase on the surface of the particles. Thus, at least for the synthetic samples, the presence of hydroxyl groups in the lattices of the haematites might be a suitable candidate to explain the behaviour observed.

The Kadan haematite is reported to be of hydrothermal origin (<200 °C) and its genesis is associated with a Tertiary fluorite–barite mineralization. Fig. 7 shows the typical weight loss pattern of a Kadan haematite sample (<40 μm) measured during continuous heating from room temperature up to 1000 °C using a constant rate of 10 °C min^{-1}. The thermogravimetric curve shows three distinct steps starting around 400, 700 and 900 °C, respectively. The weight losses at these high temperatures most probably correspond to the release of tightly held hydroxyl groups, whereas the initial decrease in weight up to ≈ 200°C can be explained by the release of more weakly bound adsorbed water. This specific thermogravimetric behaviour seems to support our hypothesis that the release of hydroxyl groups would trigger the formation of a spinel phase from pure haematite.

The genesis of LH3 haematite is not known in detail, and unfortunately, not enough sample material was left to perform thermogravimetric analysis. However, the brief description of the original ore by Dankers (1978) suggests that it was formed at relatively low temperatures because of the relative poor crystallinity compared to the other ores described by Dankers (1978) and Hartstra (1982). Furthermore, no textural indications were found for the creation from a precursor mineral devoid of water, such as magnetite. Our hypothesis can thus not be rejected by these findings.

The results obtained on the various natural and synthetic samples, however, imply that the release of incorporated hydroxyl groups is not the only condition necessary for the creation of the magnetic phase to take place. Obviously some other conditions need to be fulfilled at the same time otherwise no maghemite-like phase is formed. For instance, no or hardly any magnetic phase is created on ≈1 cm large ore fragments of Kadan haematite, whereas a spinel did form on particles crushed below ≈250 μm. This probably has to do with the availability of appropriate planes to grow on. As mentioned, Kadan haematite is acicular, developed along the crystallographic *c*-axis, so the amount of suitable planes would be very low in relatively large ore fragments. On crushing, however, the length to width ratio of the individual particles substantially improves and more suited planes become available by subdividing larger particles. This may also explain why considerably more of the new magnetic phase is created on platy-developed LH3 haematite compared to acicular Kadan haematite. Thus, in the temperature range in which the hydroxyl groups are expelled, enough and sufficiently large suited planes of haematite must be available, otherwise no maghemite-like phase can be created.

The same principle probably underlies the differences in thermomagnetic behaviour obtained on the various synthetically prepared haematite samples. The individual haematite crystallites prepared from goethite, for instance, stay low in crystal perfection and size even at high temperatures. It is likely that most of the incorporated hydroxyl groups—if incorporated at all in the goethite–haematite conversion process—will already be released before well-crystallized planes of haematite become available in sufficient size to grow the maghemite on. Similar considerations hold for the fine-grained poorly crystalline haematite particles freshly precipitated from solution. On the other hand, the crystallinity and grain-size of the sample stored for a long period in the mother solution would have been increased because of Ostwald ripening; creation of the maghemite phase would now be possible. For the haematite created from the hydrated ferric nitrate salt, our hypothesis would imply that a higher concentration of internal defects becomes incorporated during a single heating step compared to repeated heating steps to increasingly higher temperatures or annealing at temperatures close to the decomposition temperature of the precursor mineral before completing the heating procedure.

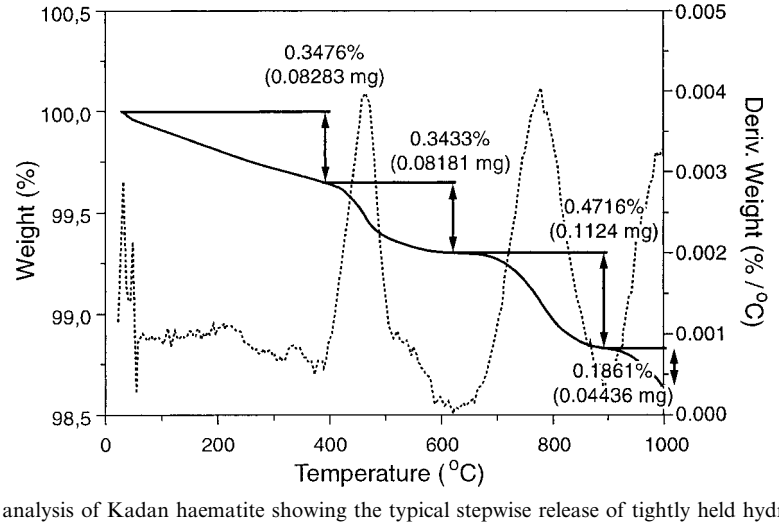

Figure 7. Thermogravimetric analysis of Kadan haematite showing the typical stepwise release of tightly held hydroxyl groups.

5 CONCLUSIONS

Trace amounts of a magnetic spinel with a characteristic T_C of 470–475 °C can be created on the surface of relatively pure haematite during a standard heating procedure in air. The spinel has a cubic structure with a unit cell length of $a = 0.8350 \pm 0.0005$ nm. It is argued that the newly created phase is a pure ferric oxide polymorph rather than an isomorphously substituted spinel. The suggested structure is that of pure maghemite with a peculiar distribution of its vacancies (and/or cations) over the two magnetic sublattices, that is, with part of the vacancies on tetrahedral interstices. A mechanism is proposed in which the structural rearrangement caused by the thermally activated release of tightly held hydroxyl groups may trigger the necessary redistribution of the oxygen framework from hcp to ccp in the outermost layers of haematite particles. The availability of well-crystallized haematite planes of appropriate size, however, seems to be an explicit condition for the epitaxial maghemite growth to take place.

ACKNOWLEDGMENTS

We gratefully acknowledge the assistance of Tom Mullender and Adry van Velzen with the low-temperature measurements on the MicroMag. Eduard Petrovský kindly made available a high-purity haematite rock sample of the Kadan hydrothermal ore deposit. This work was conducted under the programme of the Dutch national research school, the Vening Meinesz Research School of Geodynamics (VMSG).

REFERENCES

Aharoni, A., Frei, E.H. & Schieber, M., 1962. Curie point and origin of weak ferromagnetism in hematite, *Phys. Rev.,* **127,** 439–441.

Annertsen, H. & Hafner, S.S., 1973. Vacancy distribution in synthetic spinels of the series Fe_3O_4–γFe_2O_3, *Z. Kristallogr.,* **137,** 321–340.

Armstrong, R.J., Morrish, A.M. & Sawatzky, G.A., 1966. Mössbauer study of ferric ions in the tetrahedral and octahedral sites of a spinel, *Phys. Lett.,* **23,** 414–416.

Bate, G., 1980. Recording materials, in *Ferromagnetic Materials,* Vol. 2, pp. 381–507, ed. Wohlfarth, E.P., North-Holland, New York.

Bernal, J.D., Dasgupta, D.R. & Mackay, A.L., 1957. Oriented transformation in iron oxides and hydroxides, *Nature,* **180,** 645–647.

Bernal, J.D., Dasgupta, D.R. & Mackay, A.L., 1959. The oxides and hydroxides of iron and their structural inter-relationships, *Clay Min. Bull.,* **4,** 5–30.

Birks, J.B., 1950. The properties of ferromagnetic compounds at centimetre wavelengths, *Proc. Phys. Soc. Lond. B.,* **63,** 65–74.

Blackman, M. & Kaye, G., 1960. An electron diffraction study of the effects of heat treatment on αFe_2O_3 (haematite) single crystals, *Proc. Phys. Soc. Lond.,* **75,** 364–368.

Blake, R.L., Hessevick, R.E., Zoltai, T. & Finger, L.W., 1966. Refinement of the hematite structure, *Am. Min.,* **51,** 123–129.

Boudeulle, M., Batis-Landoulis, H., Leclercq, C.-H. & Vergnon, P., 1983. Structure of γFe_2O_3 microcrystals: vacancy distribution and structure, *J. Solid State Chem.,* **48,** 21–32.

Bragg, W.L., Gottfried, C. & West, J., 1931. *Z. Kristallogr.,* **77,** 255.

Braun, P.B., 1952. A superstructure in spinels, *Nature,* **27,** 1123.

Bucur, I., 1978. Experimental study of the origin and properties of the defect moment in single domain haematite, *Geophys. J. R. astr. Soc.,* **55,** 589–604.

Chevallier, R., 1951. Propriétés magnétiques de l'oxyde ferrique rhomboédrique (Fe_2O_3–α), *J. Phys. Radium,* **12,** 178–188.

Coey, J.M.D., 1987. Noncollinear spin structures, *Can. J. Phys.,* **65,** 1210–1232.

Collyer, S., Grimes, N.W., Vaughan, D.J. & Longworth, G., 1988. Studies of the crystal structure and chemistry of titanomaghemite, *Am. Min.,* **73,** 153–160.

Cornell, R.M. & Schwertmann, U., 1996. *The Iron Oxides,* VCH, New York.

Da Costa, G.M., De Grave, E., Bowen, L.H., de Bakker, P.M.A. & Vandenberghe, R.E., 1995. Temperature dependence of the hyperfine parameters of maghemite and Al-substituted maghemites, *Phys. Chem. Min.,* **22,** 178–185.

Dankers, P.H.M., 1978. Magnetic properties of dispersed natural iron-oxides of known grain-size, *PhD thesis,* Utrecht University, Utrecht.

Dankers, P.H.M., 1981. Relationship between median destructive field and remanent coercive forces for dispersed natural magnetite, titanomagnetite and hematite, *Geophys. J. R. astr. Soc.,* **64,** 447–461.

De Boer, C.B., 1999. Rock-magnetic studies on hematite, maghemite and combustion-metamorphic rocks. *PhD thesis,* Utrecht University, Utrecht.

De Boer, C.B. & Dekkers, M.J., 1996. Grain-size dependence of the rock magnetic properties for a natural maghemite, *Geophys. Res. Lett.,* **23,** 2815–2818.

De Boer, C.B. & Dekkers, M.J., 1998. Thermomagnetic behaviour of hematite and goethite as a function of grain size in various non-saturating magnetic fields, *Geophys. J. Int.,* **133,** 541–552.

Dekkers, M.J., 1990. Magnetic properties of natural goethite—III. Magnetic behaviour and properties of minerals originating from goethite dehydration during thermal demagnetization, *Geophys. J. Int.,* **103,** 233–250.

Dekkers, M.J. & Rochette, P., 1992. Magnetic properties of chemical magnetisation in synthetic and natural goethite: prospects for a natural remanent magnetisation/thermoremanent magnetisation ratio paleomagnetic stability test? *J. geophys. Res.,* **97,** 17 291–17 307.

Dunlop, D.J., 1971. Magnetic properties of fine-particle hematite, *Ann. Géophys.,* **27,** 269–293.

Dunlop, D.J. & Özdemir, Ö., 1997. *Rock Magnetism—Fundamentals and Frontiers,* Cambridge University Press, Cambridge.

Dzyaloshinsky, I.E., 1958. A thermodynamic theory of 'weak' ferromagnetism of antiferromagnetics, *J. Phys. Chem. Solids,* **4,** 241–255.

Eggleton, R.A., Schulze, D.G. & Stucki, J.W., 1988. Introduction to crystal structures of iron-containing minerals, in *Iron in Soils and Clay Minerals,* NATO ASI Series C217, pp. 141–164., eds Stucki, J.W., Goodman, B.A., & Schwertmann, U., D. Riedel, Dordrecht.

Finch, G.I. & Sinha, K.P., 1957. An electron-diffraction study of the transformation αFe_2O_3 to γFe_2O_3, *Proc. R. Soc. Lond. A.,* **241,** 1–8.

Flanders, P.J. & Remeika, J.P., 1965. Magnetic properties of hematite single crystals, *Phil. Mag.,* **11,** 1271–1288.

Frölich, F. & Vollstädt, H., 1967. Untersuchungen zur Bestimmung der Curietemperatur von Maghemit (γFe_2O_3), *Monatsber. Deutsch. Akad. Wiss., Berlin,* **9,** 180–186.

Fysh, S.A. & Clark, P.E., 1982. Aluminous hematite: a Mössbauer study, *Phys. Chem. Min.,* **8,** 257–267.

Gallagher, P.K. & Gyorgy, E.M., 1969. Morin transition and lattice spacing of hematite as a function of particle size, *Phys. Rev.,* **180,** 622.

Gardner, R.F.G., Sweett, F. & Tanner, D.W., 1963. The electrical properties of alpha ferric oxide—I. The impure oxide, *J. Phys. Chem. Solids,* **24,** 1175–1183.

Goss, C.J., 1988. Saturation magnetisation, coercivity and lattice parameter changes in the system Fe_3O_4–γFe_2O_3, and their relationship to structure, *Phys. Chem. Min.,* **16,** 164–171.

Greaves, C., 1983. A powder neutron diffraction investigation of vacancy ordering and covalency in γFe_2O_3, *J. Solid State Chem.,* **49,** 325–333.

Haigh, G., 1957. Observations on the magnetic transition in hematite at −15 °C, *Phil. Mag.,* **2,** 877–890.

Haneda, K. & Morrish, A.H., 1977. Vacancy ordering in γFe_2O_3 small particles, *Solid State Commun.,* **22,** 779–782.

Hartstra, R.L., 1982. Some rockmagnetic parameters for natural iron-titanium oxides. *PhD thesis,* Utrecht University, Utrecht.

Heider, F. & Dunlop, D., 1987. Two types of chemical remanent magnetization during the oxidation of magnetite, *Phys. Earth planet. Inter.,* **46,** 24–45.

Hejda, P., Kropácek, V., Petrovský, E., Zelinka, T. & Žatecký, J., 1992. Some magnetic properties of synthetic and natural hematite of different grain size, *Phys. Earth planet. Inter.,* **70,** 261–272.

Johnson, H.P. & Merrill, R.T., 1974. Low-temperature oxidation of a single-domain magnetite, *J. geophys. Res.,* **79,** 5533–5534.

Kachi, S., Momiyami, G. & Shimizu, S., 1963. An electron diffraction study and a theory of the transformation from γFe_2O_3 to αFe_2O_3, *J. Phys. Soc. Japan,* **18,** 106–116.

Lindsley, D.H., 1976a. The crystal chemistry and structure of oxide minerals as exemplified by the Fe–Ti oxides, in *Oxide Minerals, Reviews in Mineralogy,* Vol. 3, pp. L1–60, ed. Rumble, D., Mineral Society America, Washington D.C.

Lindsley, D.H., 1976b. Experimental studies of iron oxide minerals, in *Oxide Minerals, Reviews in Mineralogy,* Vol. 3, pp. L61–88, ed. Rumble, D., Mineral Society America, Washington D.C.

Maxwell, L.R., Smart, J.S. & Brunaver, S., 1949. Dependence of the intensity of magnetization and the Curie point of certain iron oxides upon ratio of Fe^{2+}/Fe^{3+}, *Phys. Rev.,* **76,** 459–460.

Meillon, S., Dammak, H., Flavin, E. & Pascard, H., 1995. Existence of a direct phase transformation from haemite to maghemite, *Phil. Mag. Lett.,* **72,** 105–110.

Michel, A. & Chaudron, G., 1935. Étude du sesquioxide de fer cubique stabilisé, *C. R. Acad. Sci. Paris,* **201,** 1191–1193.

Morrish, A.H., 1994. *Canted Antiferromagnetism: Hematite,* World Scientific, London.

Moskowitz, B.M., 1993. High-temperature magnetostriction of magnetite and titanomagnetites, *J. geophys. Res.,* **98,** 359–372.

Mullender, T.A.T., van Velzen, A.J. & Dekkers, M.J., 1993. Continuous drift correction and separate identification of ferrimagnetic and paramagnetic contribution in thermomagnetic runs, *Geophys. J. Int.,* **114,** 663–672.

Néel, L., 1948. Propriétés magnétiques des ferrites: ferrimagnétisme et antiferromagnétisme, *Ann. Phys.,* **3,** 137–198.

Nininger, R.C. & Schroeer, D., 1978. Mössbauer studies of the Morin transition in bulk and microcrystalline αFe_2O_3, *J. Phys. Chem. Solids,* **39,** 137–144.

O'Reilly, W., 1968. Estimation of the Curie temperatures of maghemite and oxidized titanomaghemites, *J. Geomag. Geoelectr.,* **20,** 381–386.

O'Reilly, W., 1984. *Rock and Mineral Magnetism,* Blackie, Glasgow.

Özdemir, Ö., 1990. High-temperature hysteresis and thermoremanence of single-domain maghemite, *Phys. Earth planet. Inter.,* **65,** 125–136.

Özdemir, Ö., 1998. Chemical remanent magnetization during the transformation of goethite to hematite: possible formation of intermediate spinel product, *Geol. Carpathica,* **49,** 225 (abstract).

Özdemir, Ö. & Banerjee, S.K., 1984. High-temperature stability of maghemite, *Geophys. Res. Lett.,* **11,** 161–164.

Özdemir, Ö. & Dunlop, D.J., 1988. Crystallization remanent magnetization during the transformation of maghemite to hematite, *J. geophys. Res.,* **93,** 6530–6544.

Pecharromán, C., Gonzáles-Carreño, T. & Iglesias, J.E., 1995. The infrared dielectric properties of maghemite, γFe_2O_3, from reflectance measurement on pressed powders, *Phys. Chem. Min.,* **22,** 21–29.

Petrovský, E., Dekkers, M.J., Kropácek, V., Hejda, P. & Zelinka, T., 1994. Incompatible magnetic behaviour of fine-grained natural hematite samples prepared in similar ways, *Studia Geophys. Geod.,* **38,** 46–56.

Petrovský, E., Kropácek, V., Dekkers, M.J., de Boer, C., Hoffmann, V. & Ambatiello, A., 1996. Transformation of hematite to maghemite as observed by changes in magnetic parameters: effects of mechanical activation?, *Geophys. Res. Lett.,* **23,** 1477–1480.

Ramdani, A., Steimetz, J., Gleitzer, C., Coey, J.M.D. & Friedt, J.M., 1987. Perturbation de l'echange electronique rapide par des lacunes cationiques dans $Fe_{3-x}O_4$ ($x \leq 0.09$), *J. Phys. Chem. Solids,* **48,** 217–228.

Readman, P.W. & O'Reilly, W., 1972. Magnetic properties of oxidized (cation-deficient) titanomaghemite, $(Fe, Ti, \square)_3O_4$, *J. Geomag. Geoelctr.,* **24,** 69–90.

Schwertmann, U. & Cornell, R.M., 1991. *Iron Oxides in the Laboratory,* VCH, Weinheim.

Schwertmann, U. & Murad, E., 1990. The influence of aluminium on iron oxides: XIV, Al-substituted magnetite synthesized at ambient temperatures, *Clays Clay Min.,* **38,** 196–202.

Shull, C.G., Strauser, W.A. & Wollan, E.O., 1951. Neutron diffraction by paramagnetic and antiferromagnetic substances, *Phys. Rev.,* **83,** 333–345.

Smit, J. & Wijn, H.P.J., 1959. *Ferrites,* Philips' Technical Library, Eindhoven.

Smith, P.K.K., 1979. The observation of enantiomorphous domains in a natural maghemite, *Contrib. Mineral. Petrol.,* **69,** 249–254.

Stanjek, H. & Schwertmann, U., 1992. The influence of aluminum on iron oxides, Part XVI: hydroxyl and aluminium substitution in synthetic hematites, *Clays Clay Min.,* **40,** 347–354.

Stocking, L.B. & Tauxe, L., 1990. Properties of chemical remanence in synthetic hematite: Testing theoretical predictions, *J. geophys. Res.,* **95,** 12 639–12 652.

Šubrt, J., Šolcavá, A., Hanousek, F., Petrina, A. & Zapletal, V., 1984. Preparation of αFe_2O_3 (hematite) by oxidation precipitation of aqueous solutions of iron (II) sulphate, *Collection Czechslovak Chem. Commun.,* **49,** 2478–2485.

Takei, H. & Chiba, S., 1966. Vacancy ordering in epitaxially-grown single crystals of γ-Fe_2O_3, *J. Phys. Soc. Japan,* **21,** 1255–1263.

Van Oorschot, I.H.M. & Dekkers, M.J., 1999. Dissolution behaviour of fine-grained magnetite and maghemite in the citrate–bicarbonate–dithionite extraction method, *Earth planet Sci, Lett.,* **167,** 283–295.

Van Oosterhout, G.W. & Rooijmans, C.J.M., 1958. A new superstructure in gamma-ferric oxide, *Nature,* **181,** 44.

Waychunas, G.A., 1991. Crystal chemistry of oxides and oxyhydroxides, in *Oxide Minerals, Review in Mineralogy,* Vol. 25, pp. 11–68, ed. Lindsley, D.H., Mineral Society America, Washington, DC.

Weber, H.P. & Hafner, S.S., 1971. Vacancy distribution in non-stoichiometric magnetites, *Z. Kristallogr.,* **133,** 327–340.

Wilson, R.L., 1961. Paleomagnetism in Northern Ireland, I: The thermal demagnetization of natural magnetic moments in rocks, *Geophys. J. R. astr. Soc.,* **5,** 45–58.

Wolska, E., 1981. The structure of hydrohematite, *Z. Kristallogr.,* **154,** 69–75.

Wolska, E. & Schwertmann, U., 1989. Nonstoichiometric structures during dehydroxylation of goethite, *Z. Kristallogr.,* **189,** 223–237.

Zdujic, M., Jovalekic, C., Karanovic, Lj, Mitric, M., Poleti, D. & Skala, D., 1998. Mechanochemical treatment of α-Fe_2O_3 powder in air atmosphere, *Materials Sci. Eng.,* **A245,** 109–117.